ISSN 1063-7761, Journal of Experimental and Theoretical Physics, 2016, Vol. 123, No. 3, pp. 373–381. © Pleiades Publishing, Inc., 2016.
Original Russian Text © V.S. Gorelik, V.V. Kapaev, 2016, published in Zhurnal Eksperimental'noi i Teoreticheskoi Fiziki, 2016, Vol. 150, No. 3, pp. 435–444.

ATOMS, MOLECULES, OPTICS

Electromagnetic-Field Amplification in Finite One-Dimensional Photonic Crystals

V. S. Gorelik[a] and V. V. Kapaev[a, b,*]

[a] *Lebedev Physics Institute, Russian Academy of Sciences, Moscow, 119991 Russia*
[b] *MIET National Research University, Moscow, 124498 Russia*
**e-mail: kapaev@sci.lebedev.ru*

Received December 30, 2015

Abstract—The electromagnetic-field distribution in a finite one-dimensional photonic crystal is studied using the numerical solution of Maxwell's equations by the transfer-matrix method. The dependence of the transmission coefficient T on the period d (or the wavelength λ) has the characteristic form with $M-1$ (M is the number of periods in the structure) maxima with $T=1$ in the allowed band of an infinite crystal and zero values in the forbidden band. The field-modulus distribution $E(x)$ in the structure for parameters that correspond to the transmission maxima closest to the boundaries of forbidden bands has maxima at the center of the structure; the value at the maximum considerably exceeds the incident-field strength. For the number of periods $M \sim 50$, more than an order of magnitude increase in the field amplification is observed. The numerical results are interpreted with an analytic theory constructed by representing the solution in the form of a linear combination of counterpropagating Floquet modes in a periodic structure.

DOI: 10.1134/S1063776116070062

1. INTRODUCTION

The manufacturing of composite dielectric and semiconductor materials with controllable optical properties is an important problem of present-day physics. One-dimensional layered structures with periodically alternating refractive indices n_1 and n_2 are of great interest. Such media that contain a rather large number of layers are called one-dimensional photonic crystals [1–4]. Periodic layered structures with periods comparable to visible-spectrum wavelengths (0.4–0.8 μm) are of the most interest. The spectra of such crystals exhibit so-called stop bands, regions of strong reflection of light. The spectral position of stop bands depends on the refractive index of the layers, the period of the corresponding crystal lattice and the angle of incidence of radiation on the crystal surface. By changing these parameters, it is possible to control the optical properties of such materials. Theoretical analysis predicts a considerable change in the parameters of electromagnetic waves due to a drastic slowing of their group velocity and a corresponding increase in the spectral energy density.

Opal matrices are one important example of nanocomposite photonic crystals, viz., artificial opals constructed from densely packed silicone oxide globules [5–9]. The structure of artificial opals belongs to the face-centered cubic crystal lattice. The [111] direction of such a lattice corresponds to the growth direction and is characterized by the most perfect periodic structure. The optical properties of an opal matrix in the [111] direction are close to these of a one-dimensional photonic crystal. In this case, the fraction of a three-dimensional photonic crystal filled with air is 0.26. The period of the corresponding one-dimensional photonic structure typically lies in the range from 200 to 400 nm and is retained for many layers (more than 100).

The technology has also developed for manufacturing one-dimensional mesoporous photonic-crystal films based on the anode etching of doped silicon or aluminum [10, 11]. As a result, photonic-crystal films are formed that contain layers with different porosities that retain the periodicity of the corresponding one-dimensional crystal lattice. In this paper, we obtain the quantitative characteristics of electromagnetic waves near the edges of stop bands of one-dimensional photonic crystals and find conditions for the amplification of electromagnetic waves depending on the structure period and the values of the refractive indices in the alternating layers.

2. TRANSFER-MATRIX METHODS FOR A LAYERED PERIODIC STRUCTURE

It has been shown [12] that pulsed laser annealing of CdS produces a layered periodic structure in the disturbed surface region of the CdS in which the electric-field strength can considerably increase, resulting in an increase in the annealing efficiency during sub-

sequent laser pulses. In this case, the modulation period of the refractive index n is determined by the excitation wavelength. It was shown that for a weakly modulated refractive index, the system is found near the edge of the forbidden zone (stop band). In this case, the interaction of counterpropagating Flouqet modes leads to the field amplification in the structure.

In this paper, we analyze the possibility of obtaining such effects when an electromagnetic wave is incident on a one-dimensional photonic crystal or a finite photonic-crystal film with the periodic modulation $n(x)$. Maxwell's equation for the electric vector of a normally incident electromagnetic wave has the form

$$\frac{d^2E}{dx^2} + \left[\frac{2\pi}{\lambda}n(x)\right]^2 E = 0, \tag{1}$$

where λ is the radiation wavelength in a vacuum, $n(x)$ is a periodic function with period d for a region restricted by the interval $[0, L]$ ($L = Md$, and M is the number of periods). Consider the function $n(x)$ in the step form

$$\begin{aligned} n(x) &= n_1 \quad \text{at} \quad id < x < id + l_1, \\ n(x) &= n_2 \quad \text{at} \quad id + l_1 < x < (i+1)d, \end{aligned} \tag{2}$$

where the period number $i = 0, 1, \ldots, M-1$, l_1 is the width of a region with the refractive index n_1, and $l_2 = d - l_1$ is the width of a region with the refractive index n_2. In each region with a constant n, the solution of (1) can be written in the form

$$E_j = A_j e^{ik_j(x-x_j)} + B_j e^{-ik_j(x-x_j)}, \tag{3}$$

where x_j is the left boundary of the jth layer. Below, we restrict ourselves to the normal incidence when $k_j = 2\pi n_j/\lambda$. When the wave is incident from the left in the region $x < 0$ the field has the form

$$E = e^{ik_0x} + re^{-ik_0x}, \tag{4}$$

while for $x > L$,

$$E = te^{ik_0x}. \tag{5}$$

We will find the coefficients A_j and B_j, as well as the reflection and transmission coefficients r and t, using the transfer-matrix method.

By joining the fields and their derivatives at the boundary of the layers j and $j+1$, we obtain the relationship of the coefficients A_{j+1} and B_{j+1} with A_j and B_j:

$$\begin{aligned} A_{j+1} &= 0.5\left[A_j e^{ik_jh_j}\left(1 + \frac{k_j}{k_{j+1}}\right) + B_j e^{-ik_jh_j}\left(1 - \frac{k_j}{k_{j+1}}\right)\right], \\ B_{j+1} &= 0.5\left[A_j e^{ik_jh_j}\left(1 - \frac{k_j}{k_{j+1}}\right) + B_j e^{-ik_jh_j}\left(1 + \frac{k_j}{k_{j+1}}\right)\right], \end{aligned} \tag{6}$$

where h_j is the thickness of the jth layer. In the matrix form, we have

$$\begin{pmatrix} A_{j+1} \\ B_{j+1} \end{pmatrix} = \mathbf{M}_{j,j+1}\begin{pmatrix} A_j \\ B_j \end{pmatrix} = \begin{pmatrix} 0.5e^{ik_jh_j}\left(1 + \frac{k_j}{k_{j+1}}\right) & 0.5e^{-ik_jh_j}\left(1 - \frac{k_j}{k_{j+1}}\right) \\ 0.5e^{ik_jh_j}\left(1 - \frac{k_j}{k_{j+1}}\right) & 0.5e^{-ik_jh_j}\left(1 + \frac{k_j}{k_{j+1}}\right) \end{pmatrix}\begin{pmatrix} A_j \\ B_j \end{pmatrix}. \tag{7}$$

By applying (7) successively to all of the boundaries, beginning from the first one and taking into account the fact that according to (4), (5), $A_0 = 1$, $B_0 = r$ (semi-infinite layer $x < 0$), $A_{2M+1} = t$, $B_{2M+1} = 0$ (semi-infinite layer $x > L$), we obtain

$$\begin{pmatrix} t \\ 0 \end{pmatrix} = \mathbf{M}\begin{pmatrix} 1 \\ r \end{pmatrix} = \prod_j \mathbf{M}_{j,j+1}\begin{pmatrix} 1 \\ r \end{pmatrix}. \tag{8}$$

Here,

$$\mathbf{M} = \begin{pmatrix} m_{11} & m_{12} \\ m_{21} & m_{22} \end{pmatrix} \tag{9}$$

is the transfer matrix of the structure. The reflection and transmission coefficients are obtained in the form

$$\begin{aligned} r &= -\frac{m_{12}}{m_{22}}, \\ t &= \frac{m_{11}m_{22} - m_{12}m_{21}}{m_{22}} = \frac{k_1}{k_{2M+1}}\frac{1}{m_{22}}. \end{aligned} \tag{10}$$

Here,

$$m_{11}m_{22} - m_{12}m_{21} = \det\mathbf{M} = \prod_j \det\mathbf{M}_{j,j+1},$$

$$\det\mathbf{M}_{j,j+1} = \frac{k_j}{k_{j+1}}.$$

Thus, by determining r from (10) and using (6), we can calculate the electric-field distribution in the entire structure.

3. THE NUMERICAL ANALYSIS OF THE FIELD DISTRIBUTION

We consider the simplest model of a one-dimensional photonic crystal with alternating silicon oxide and air layers corresponding to the parameters of an opal matrix. We assume that $n_1 = 1.46$, $n_2 = 1$, and $n_0 = n_{2M+1} = 1$.

Figure 1 shows the typical dependence of the structure transmission $T = |t|^2$ on the period for the number of periods $M = 30$ and $l_1/d = 0.3$ obtained by the transfer-matrix method. The inset presents an enlarged region that contains the three first transmission maxima to the left of the first forbidden zone. The characteristic features of dependences $T(d)$ are the presence of a series of interference transmission maxima with $T = 1$ and regions with zero transmission (forbidden bands). The position of the boundaries of forbidden bands corresponds well to the values from the dispersion relationship for an infinite periodic structure [12, 13]:

$$\cos(kd) = \cos(k_1 l_1)\cos(k_2 l_2) - \frac{1}{2}\left(\frac{k_1}{k_2} + \frac{k_2}{k_1}\right)\sin(k_1 l_1)\sin(k_2 l_2), \quad (11)$$

where k is the Floquet wave vector. The reflection regions of the electromagnetic wave correspond to parameters for which the modulus of the right-hand side of (11) exceeds unity. The boundaries of the stop band satisfy the condition $\cos(kd) = \pm 1$, which gives $kd = \pi q$ ($q = 1$ is the first band, $q = 2$ is the second band, etc.). The number of unit transmission maxima in each allowed band is $M - 1$ under the condition $2n_1 l_1 < \lambda$. If in the range of the parameters d and λ under study the condition $2n_1 l_1 = \lambda$ is fulfilled, for which the unit transmission takes place for a structure that contains one period, then additional unit transmission maxima occur for $d/\lambda = (2n_1 l_1/d)^{-1}$.

The calculations show that the electromagnetic-field distribution in the structure for parameters that correspond to the transmission maxima is the most interesting. Figure 2 shows the dependences of the electric-field modulus E on the coordinate x for the first four maxima of $T(d)$ to the left of the first forbidden band (stop band).

The distribution $E(x)$ has a characteristic shape with field oscillations in each of the periods and a smooth envelope, with the number of maxima of the envelope E_{max} being equal to the number p of the maximum of $T(d)$ counted from the forbidden-band boundary. The dependences $E(x)$ for the transmission maxima to the right of the forbidden band and for the second and subsequent forbidden bands behave similarly. The most important issue is that the value of E_{max} exceeds the incident radiation amplitude (equal to unity) and decreases with the increasing number p of the maximum. i.e., with the distance from the forbidden band boundary.

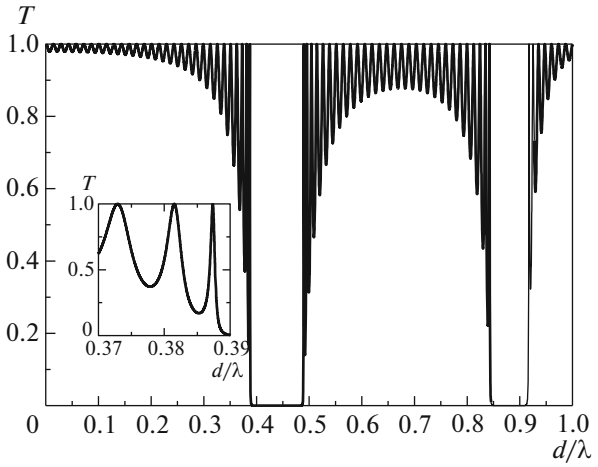

Fig. 1. The dependence of the transmission T on the period d for $n_1 = 1.46$, $M = 30$, $l_1/d = 0.3$.

To illustrate the field distribution outside the transmission maxima, Fig. 3 presents dependences $E(x)$ at the boundary of the zero-transmission band and at the first minima of the transmission $T(d)$. The maximum field strengths in this case are of the order of unity and weakly depend on the minimum number.

It is interesting to observe the behavior of the system with changing structure parameters. Figure 4 shows the dependences of the maximum amplitude E_{max} in the structure on the degree of filling l_1/d for the first maxima of $T(d)$ to the right and left of the first two forbidden bands for $M = 50$. One can see that the type of dependences $E_{max}(l_1)$ is determined by the number of the nearest forbidden band. The dependence for the first band has one maximum at $l_1 \sim 0.4d$ and for the second band two maxima at $l_1 \sim 0.2d$ and $l_1 \sim 0.65d$ and a deep minimum at $l_1 \sim 0.4d$. The field amplitude E_{max} for optimal values of l_1 is an order of magnitude higher than the incident field (two orders of magnitude for the electromagnetic energy density of the field).

We will show below that the field amplification at the center of the structure is caused by the interference of counterpropagating Floquet modes. In fact the strength of the interaction of the electromagnetic fields with a periodic structure determines the forbidden-band width in an infinite system. In this connection it is of interest to compare the dependence $E_{max}(l_1)$ with the change in the forbidden-band width $\Delta(l_1)$. Figure 5 shows the dependences of the position of the edges of the forbidden band $(d/\lambda)_c$ on the fraction of regions with the refractive index n_1 for the first two forbidden bands obtained from (11) and the corresponding widths of the first and second forbidden bands. The characteristic feature is the presence of one maximum for the width of the first forbidden band and two maximums for the second forbidden band. For

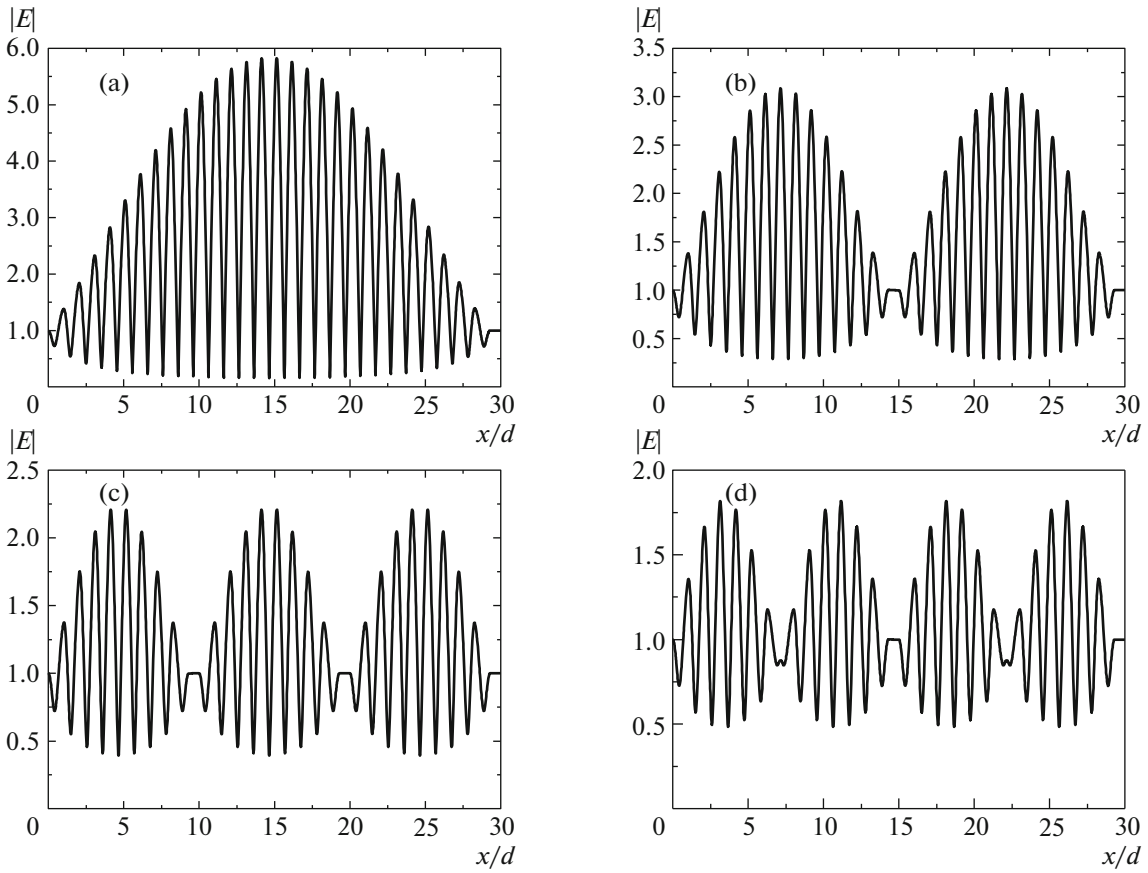

Fig. 2. The field-modulus distributions for $M = 30$ and $l_1 = 0.3d$ for the first four transmission maxima to the left of the first forbidden band (a, 1; b, 2; c, 3; d, 4); $d/\lambda = 0.387$, 0.382, 0.373, and 0.363, respectively.

$l_1/d = 0.407$, the width of the second forbidden band vanishes. For this value, the condition $k_1 l_1 = k_2 l_2$ is fulfilled and the right-hand side of (11) does not exceed unity. As a result, the even forbidden bands determined by the condition $\cos kd = 1$ contract to a point. By comparing Figs. 4 and 5, we see that the maximum field amplitude for a finite structure is observed for parameters that correspond to the maximum widths of the corresponding forbidden band, while the minimum of E_{max} for $l_1 \sim 0.4d$ corresponds to the elimination of the width of the second forbidden band.

Figure 6 shows the dependences of E_{max} on the number M of periods in the structure. The characteristic feature is a linear increase in the amplitude with the structure size. The increase in the amplitude is caused by the interference of waves reflected from interfaces and sample boundaries. The interference pattern is formed due to multiple propagations of a wave in the structure, i.e., the previous consideration is correct if the coherence length considerably exceeds the sample length. In addition, as M increases, the distance $T(d)$ between the maxima decreases and, for a finite linewidth of exciting radiation, the total pattern is obtained due to averaging over the wavelengths. This will stop the growth for some length of the structure. The field amplification is also suppressed by absorption in the system. The influence of absorption will increase with increasing M and the field maximum will decrease with increasing M.

Along with the field strength at the maxima, the field distribution over the period in regions of the envelope maxima is of interest for particular applications of this phenomenon. Figure 7 shows such a distribution for the first transmission maxima to the right and left of the first two forbidden bands. The general characteristics are as follows. The number of the local maxima of $|E|$ within one period is equal to the number of the nearest forbidden band; for the first stop band, for the left maximum of T, in each of the periods the maximum of $|E|$ is located in a dielectric layer; for the left one it is located in a vacuum. For the second and third bands, one of the maxima behaves similarly, but additional maxima located in a vacuum occur (for the given filling degree). Thus, by choosing the value of the period (or the wavelength), we can provide the required position of the field-intensity maximum in the structure. As noted above, variations in the field modulus at the maxima considerably depend on the degree of period filling with a dielectric l_1/d.

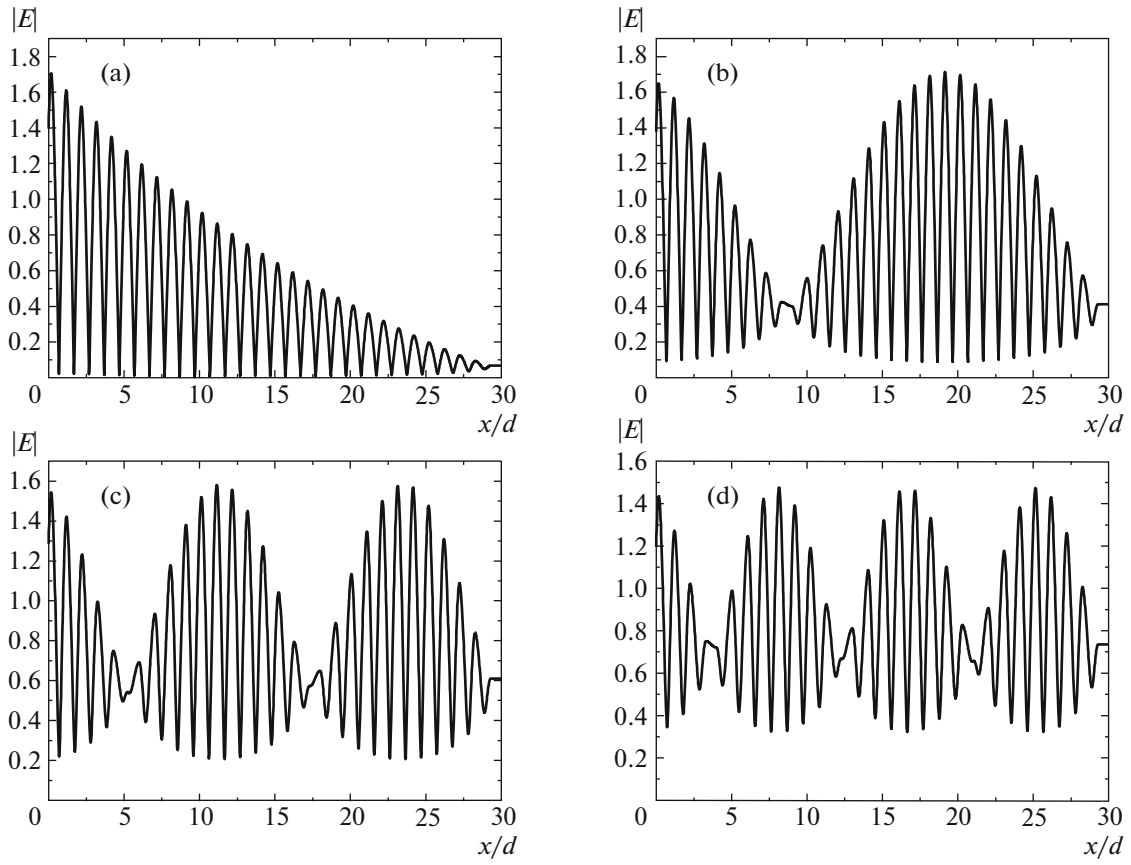

Fig. 3. The field distributions for $M = 30$ and $l_1 = 0.3$ near the zero transition threshold $d = 0.39\lambda$ (a) and in the first transmission minima $d/\lambda = 0.385$ (b), 0.378 (c), 0.368 (d).

We studied the dependences of the maximum field strength E_{max} in the structure on the refractive index n_1. The type of these dependences is determined by the value of l_1 and can be substantially different for the transmission extrema nearest to the first and second bands. Figure 8 presents dependences $E_{max}(n_1)$ for two values of l_1. For maxima located near the first forbidden band, these dependences either monotonically increase, tending to saturation for large n_1 both for the right and left maxima of T (curves *5*, *6* in Fig. 8), or monotonically increase (curve *1*) for the left maxima of T, and curves with a weak maximum for the left maxima (curve *2*). The former situation occurs for small l_1 and the latter occurs for large l_1.

For the T maxima to the right and left of the second forbidden band, the regularities are more complicated. For large $l_1 > 0.5d$, the behavior of $E_{max}(n_1)$ is quite similar to the case of the maxima located near the first forbidden band (curves *3* and *4*). For smaller l_1, a deep minimum is observed for some value of n_1 at which $E_{max} \sim 1$ (curves *7* and *8*). The position of this minimum corresponds to the vanishing of the width of the second forbidden band. As n_1 changes from 1 to 3, the value of l_1/d changes from 0.5 to 0.25. The deep minima of $E_{max}(n_1)$ are observed in this range of l_1. For $l_1 < 0.25d$, a minimum is absent and dependences $E_{max}(n_1)$ for the right and left T maxima have a weak maximum of the type of curve *4* in Fig. 8. The position of this maximum correlates with the width of the forbidden band.

4. EXPANSION OF THE SOLUTION IN FLOQUET MODES

For the periodic structure considered above, at least for large enough M and in condinion of $T = 1$, as in [12], we can use the Floquet theorem and seek a solution for $0 < x < L$ as a combination of counterpropagating Floquet modes:

$$E(x) = C_+u(x)e^{ikx} + C_-v(x)e^{-ikx}, \qquad (12)$$

where u and v are periodic functions with period d and k is the wave vector determined from (11). Coefficients C_+, C_-, r, and t can be determined from the continuity of the field and its derivative for $x = 0$ and $x = L$. We will not solve this problem completely and consider only the situation that corresponds to the transmission maximum in the previous problem, when $|t| = 1$,

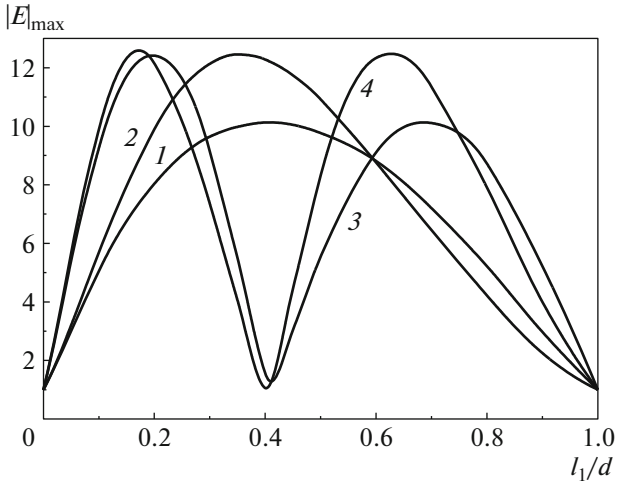

Fig. 4. The dependence of the field modulus maximum $E_{\max}$ on the region width l_1 with $n_1 = 1.46$ for $M = 50$; curves *1* and *2* correspond to the first forbidden band, curves *3* and *4* correspond to the second forbidden band.

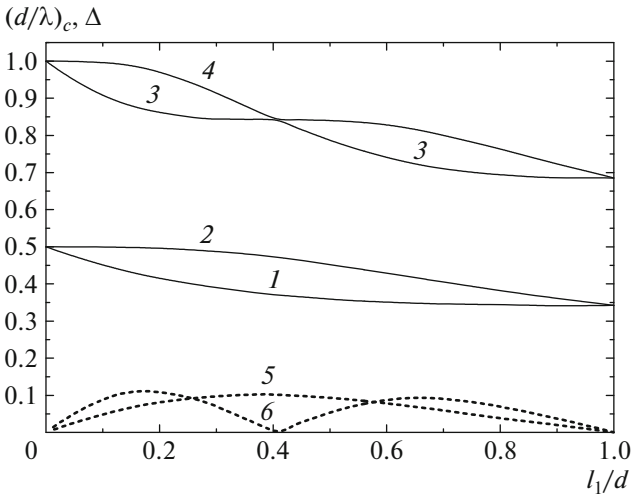

Fig. 5. The positions of the edges of the first (*1*, *2*) and second (*3*, *4*) bands and the widths of the first (*5*) and second (*6*) forbidden bands for a superlattice with $n_1 = 1.46$, and $n_2 = 1$ as functions of the filling degree l_1.

because it is under this condition that the most interesting results are obtained.

Using (12), the field in the jth period can be written in the form

$$E(x + jd) = E_+(x)e^{ikjd} + E_-(x)e^{-ikjd}, \qquad (13)$$

where j is the period number and

$$E_+(x) = C_+u(x)e^{ikx}, \quad E_-(x) = C_+v(x)e^{-ikx}.$$

The field for $x = L$ is obtained for $j = M$, $x = 0$

$$E(Md) = e^{ikMd}(E_+(0) + E_-(0)e^{-2ikMd}). \qquad (14)$$

The condition $|t| = 1$ corresponds to $|E(Md)| = |E(0)|$, and as follows from (14), it is fulfilled if

$$2kMd = 2\pi m. \qquad (15)$$

For the first allowed band, $kd < \pi$; therefore, relation (15) will be fulfilled for $M - 1$ values of m ($m = M - 1$, $M - 2$, ..., 1). For the second allowed band, $\pi < kd < 2\pi$ and (15) is also fulfilled for $M - 1$ values of m ($m = M + 1$, ..., $2M - 1$). The same number of unit maxima will also occur in subsequent allowed bands. This coincides with the results of the numerical transfer matrix calculations obtained earlier (see Fig. 1).

It was shown in [14, 15] that expressions for the transmission T and reflection R for a finite layered periodic structure can be written in the explicit form using the unimodularity of the transfer matrix for one period. The analysis of expressions for T and R showed [15] that a finite structure in each allowed band of an infinite lattice contains $M - 1$ transmission maxima, with the value of T in the maximum being unity. Thus, our results are consistent with those obtained in [14].

As shown above, structures with transmission maxima nearest to the boundaries of forbidden bands are of most interest. Therefore, it is convenient to count the numbers of maxima T from band boundaries and to introduce quantities $p = M - m$ instead of m for the states near the first forbidden band at the left, $p = m - M$ at the right, and $p = \pm(2M - m)$ for the second band. (the plus and minus signs correspond to the

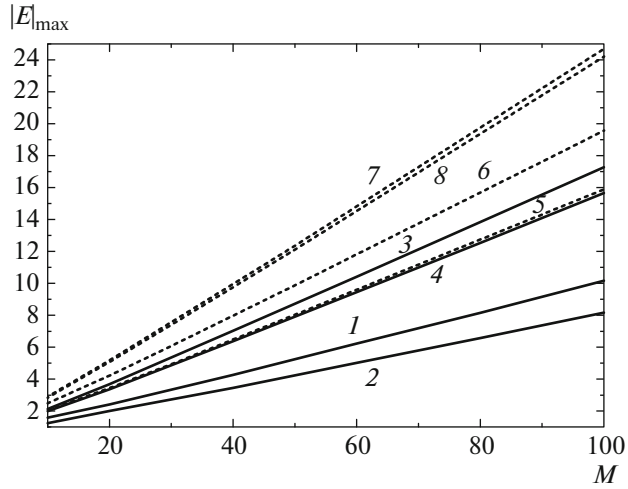

Fig. 6. The dependences of the maximum electric field on the number M of periods for the first transmission maxima near the edges of the first (*1*, *5* at the left, *2*, *6* at the right) and second (*3*, *7* at the left, *4*, *8* at the right) forbidden bands. $n_1 = 1.46$, $l_1 = 0.8d$ (solid curves *1*–*4*) and $l_1 = 0.2d$ (dashed curve *5*–*8*).

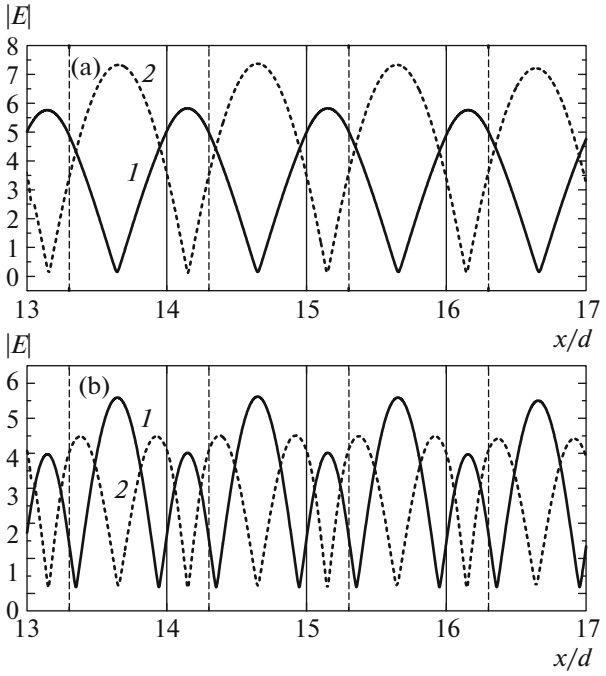

Fig. 7. The field modulus distributions in a structure with $n_1 = 1.46$, $l_1 = 0.3$ and $M = 30$. The solid curves correspond to the first transmission maximum at the left, the dashed curves correspond to the first transmission maximum to the right of the first (a) and second (b) forbidden band.

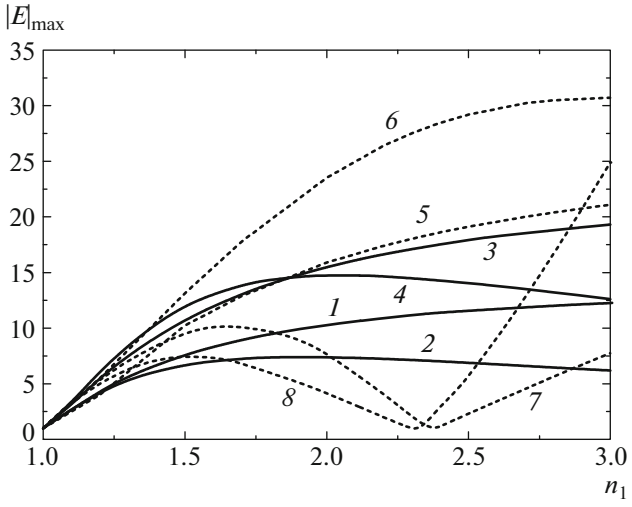

Fig. 8. The dependences of the maximum field strength on the refractive index n_1 for $M = 50$, $l_1 = 0.7d$ (curves *1*–*4*) and $l_1 = 0.3d$ (curves *5*–*8*) for the first maxima of T near the first (*1*, *2*, *5*, *6*) and second (*3*, *4*, *7*, *8*) forbidden bands.

states at the left and right of the forbidden band, respectively). Then, we obtain from (15) that the subsequent transmission maxima will be observed for

$$kd = \pi(1 \pm p/M) \tag{16}$$

for the first band and

$$kd = \pi(2 \pm p/M) \tag{17}$$

for the second band ($p = 1, 2, \ldots$ is the number of the maximum). By substituting (16) and (17) into dispersion equation (11), we obtain the position d_c of the transmission maxima, which coincides with good accuracy with the positions from numerical calculations (Fig. 1).

As follows from (12), the total field intensity in the medium is a combination of oscillating functions with periods d and $d_1 = d/(1 - p/M)$ (for the first allowed band). The resulting intensity (and the field modulus) is the beats of two oscillations with close frequencies. It can be shown that the largest beat period is determined by the condition $D = Md = (M - p)d_1$ and coincides with the structure length L. For $p = 2$ and even M, $D/2$ is also a period for the intensity. For odd M, $D/2$ will not be a strict period, but nevertheless a structure with $D/2$ will be distinctly observed in the field envelope. Similarly, for $p = 3$ a structure with $D/3$ will be observed, etc. These considerations explain the dependences $E(x)$ presented in Fig. 2. Thus, simple considerations based on the Floquet theorem allow us to explain the main features of the behavior of the field in a finite layered periodic structure.

Let us find the field distribution $E(x)$ at the maxima $t(d)$ by the Floquet method. In the interval $[0, d]$, the solution for each of the Floquet modes can be written in the form

$$\begin{aligned} E_{\pm}^{f}(x) &= C_1 e^{ik_1 x} + D_1 e^{-ik_1 x} \quad \text{at} \quad 0 < x < l_1, \\ E_{\pm}^{f}(x) &= C_2 e^{ik_2(x-l_1)} + D_2 e^{-ik_2(x-l_1)} \quad \text{at} \quad l_1 < x < d. \end{aligned} \tag{18}$$

Using the Floquet theorem in the form $E_{\pm}(x + d) = E_{\pm}(x)e^{\pm ikd}$, we write the solution in the interval $d < x < d + l_1$ in terms of the coefficients C_1 and D_1. By joining the field and its derivatives for $x = l_1$ and $x = d$, we obtain the system of linear equations for C_i and D_i:

$$\begin{pmatrix} e^{ik_1 l_1} & e^{-ik_1 l_1} & -1 & -1 \\ k_1 e^{ik_1 l_1} & -k_1 e^{-ik_1 l_1} & -k_2 & k_2 \\ e^{ikd} & e^{ikd} & -e^{ik_2 l_2} & -e^{-ik_2 l_2} \\ k_1 e^{ikd} & -k_1 e^{ikd} & -k_2 e^{ik_2 l_2} & k_2 e^{ik_2 l_2} \end{pmatrix} \times \begin{pmatrix} C_1 \\ D_1 \\ C_2 \\ D_2 \end{pmatrix} = \begin{pmatrix} 0 \\ 0 \\ 0 \\ 0 \end{pmatrix}. \tag{19}$$

The equality of the determinant of this system to zero gives the dispersion equation (11). By using the first three equations of system (19), we can express the coefficients in terms of one of them, for example, C_1. However, we will proceed differently, requiring the fulfillment of the condition $E(0) = 1$ (this corresponds to $C_1 + D_1 = 1$ and $r = 0$). In this case, the expressions for the coefficient have the form

$$\begin{aligned} C_1 &= 0.5 + i(-k_1\sin(k_1l_1)\sin(k_2l_2) \\ &+ k_2\cos(k_1l_1)\cos(k_2l_2) - k_2y)/H, \\ D_1 &= 0.5 + i(k_1\sin(k_1l_1)\sin(k_2l_2) \\ &- k_2\cos(k_1l_1)\cos(k_2l_2) + k_2y)/H, \\ C_2 &= (k_2y\sin(k_1l_1) + k_1\sin(k_2l_2) \\ &+ i(k_1\cos(k_2l_2) - k_1y\cos(k_1l_1)))/H, \\ D_2 &= (k_2y\sin(k_1l_1) + k_1\sin(k_2l_2) \\ &- i(k_1\cos(k_2l_2) - k_1y\cos(k_1l_1)))/H, \end{aligned} \quad (20)$$

where

$$\begin{aligned} y &= e^{ikd}, \\ H &= 2(k_2\sin(k_1l_1)\cos(k_2l_2) \\ &+ k_1\cos(k_1l_1)\sin(k_2l_2)). \end{aligned} \quad (21)$$

For the second (counterpropagating) Floquet mode, the coefficients C and D are obtained from (20) by replacing k with $-k$. It is easy to see that $C_1(k) = D_1^*(-k)$, $C_2(k) = D_2^*(-k)$, i.e., solutions for counterpropagating Floquet modes are complex conjugate, $E_+(x) = E_-^*(x)$. The total solution can be written in the form

$$E(x + jd) = c_f E_+^f(x)e^{ikjd} + c_b E_-^f(x)e^{-ikjd}. \quad (22)$$

In the case of the unit transmission ($r = 0$) under study, expressions for coefficients c_f and c_b at counterpropagating Flouqet modes are obtained from the conditions of conjugation with the incident wave on one boundary $x = 0$:

$$\begin{aligned} c_f &= \frac{1}{2k_1k_2(\sin kd)}[k_1k_2\sin(kd) + k_2^2\sin(k_1l_1) \\ &\times\cos(k_2l_2) + k_1k_2\cos(k_1l_1)\sin(k_2l_2) \\ &+0.5i((k_1^2 - k_2^2)\sin(k_1l_1)\sin(k_2l_2))], \\ c_b &= 1 - c_f. \end{aligned} \quad (23)$$

According to (22), the field at the maximum is proportional to c_f. As mentioned above, kd at the transmission maxima is determined by relationships (16) and (17). For M large enough and small p, we can expand $\sin kd$ into a series in the denominator of c_f in (23) to obtain

$$c_f \propto M/p. \quad (24)$$

This explains both a linear increase in the maximum field in the structure with increasing M (Fig. 6) and a decrease in the maximum field with an increase in the number p of the maximum (Fig. 2).

The numerical value of E_{max} can be determined from the solution in the interval $[0, d]$. Let us write $E_\pm$ in the form

$$E_\pm = \rho_\pm e^{i\varphi_\pm}, \quad (25)$$

where ρ and φ are the wave amplitude and phase. Then, the field in the jth period can be written in the form

$$E(x + jd) = e^{i(\varphi_+ + kjd)}(\rho_+ + \rho_- e^{i[(\varphi_- - \varphi_+) + 2\pi jp/M]}). \quad (26)$$

For large enough M, the phase is $\varphi_- - \varphi_+ \approx \pi$. Therefore, the field maximum will be achieved when the condition

$$2jp/M = 1 \quad (27)$$

is fulfilled. For $p = 1$, we obtain $j = M/2$. In this case, the field amplitude in this period has the form

$$|E(x + jd)| = |E_+(x) - E_-(x)|. \quad (28)$$

Thus, it is possible to calculate E_{max} and the field distribution in a layer corresponding to the maximum field based on calculations for one first period.

5. CONCLUSIONS

Based on the numerical solution of Maxwell's equations by the transfer-matrix method, the features of the transmission coefficients and field distribution in a finite layered periodic structure have been analyzed. The field-modulus distribution $E(x)$ in the structure for parameters that correspond to the transmission maxima closest to the boundaries of forbidden bands has a number of features. It was shown that the field strength at the center of the structure for the transmission maximum closest to the forbidden band can be more than an order of magnitude higher than the incident field amplitude E_0. For the subsequent transmission maxima $p = 2, 3, \ldots$, the envelope $E(x)$ is close to a periodic function with period M/p, while E_{max} decreases with the number p (for $p = 4$, $E_{max}/E_0 \sim 2$). E_{max} linearly increases with M and for $M = 50$ the field excess exceeds ten times (in this case, the electromagnetic-field energy density increases more than two orders of magnitude). The dependence of E_{max} on the system parameters has been studied. The amplification of the electromagnetic field is maximal for the filling degree l_1/d corresponding to the maximum of the width of forbidden bands of an infinite structure (approximately 0.4 for the first and 0.2 and 0.65 for the second band).

To interpret the numerical results, we constructed an analytic theory based on the representation of the solution as a linear combination of counterpropagating Floquet modes of a periodic structure. In this case, the total field intensity is a combination of oscillating functions with similar periods d and $d_1 = d/(1 - p/M)$ (p is the number of the transmission maximum). The resulting intensity (and field modulus) is the beats of two oscillations with similar frequencies, which explains the features of the $E(x)$ distribution.

REFERENCES

1. V. P. Bykov, Sov. Phys. JETP **35**, 269 (1972).
2. E. Yablonovitch, Phys. Rev. Lett. **58**, 2059 (1987).
3. S. John, Phys. Rev. Lett. **58**, 2486 (1987).
4. V. S. Gorelik, Quantum Electron. **37**, 409 (2007).
5. V. N. Astratov, V. N. Bogomolov, A. A. Kaplyanskii, A. V. Prokofiev, L. A. Samoilovich, S. M. Samoilovich, and Yu. A. Vlasov, Nuovo Cimento **17D**, 1349 (1995).
6. V. N. Bogomolov, S. V. Gaponenko, A. M. Kapitonov, A. V. Prokofiev, A. N. Ponyavina, N. I. Silvanovich, and S. M. Samoilovich, Appl. Phys. A **63**, 613 (1996).
7. Yu. P. Voinov, V. S. Gorelik, K. I. Zaitsev, L. I. Zlobina, P. P. Sverbil', and S. O. Yurchenko, Phys. Solid State **57**, 453 (2015).
8. V. S. Gorelik, S. N. Ivicheva, Yu. F. Kargin, and V. V. Filatov, Inorg. Mater. **49**, 685 (2013).
9. V. S. Gorelik, L. S. Lepnev, and A. O. Litvinova, Inorg. Mater. **50**, 1003 (2014).
10. Liu Yisen, Chang Yi, Ling Zhiyuan, Hu Xing, and Li Yi, Electrochem. Commun. **13**, 1336 (2011).
11. S. E. Svyakhovskiy, A. I. Maydykovsky, and T. V. Murzina, J. Appl. Phys. **112**, 013106 (2012).
12. V. V. Kapaev, Sov. J. Quantum Electron. **19**, 1460 (1989).
13. M. B. Vinogradova, O. V. Rudenko, and A. P. Sukhorukov, *The Theory of Waves* (Nauka, Moscow, 1979) [in Russian].
14. A. Yariv and P. Ye, *Optical Waves in Crystals: Propagation and Control of Laser Radiation* (Mir, Moscow, 1987, Wiley, New York, 2003).
15. P. Yeh, A. Yariv, and C. Hong, J. Opt. Soc. Am. **67**, 423 (1977).

Translated by M. Sapozhnikov